Neoplasia • Vol. 6, No. 6, November/December 2004, pp. 802–812 802

www.neoplasia.com

Exposure of Human Lung Cancer Cells to 8-Chloro-Adenosine Induces G_2/M Arrest and Mitotic Catastrophe[1]

Hong-Yu Zhang[*,2], *Yan-Yan Gu*[*,2], *Zeng-Gang Li*[*], *Yu-Hong Jia*[*], *Lan Yuan*[†], *Shu-Yan Li*[*], *Guo-Shun An*[*], *Ju-Hua Ni*[*] *and Hong-Ti Jia*[*,‡]

Departments of *Biochemistry and Molecular Biology and †Peking University Medical and Health Analysis Center, Peking University Health Science Center, Xue Yuan Road 38, Beijing 100083, PR China; ‡Department of Biochemistry, Capital University of Medical Sciences, You An Men, Beijing 100054, PR China

Abstract

8-Chloro-adenosine (8-Cl-Ado) is a potent chemotherapeutic agent whose cytotoxicity in a variety of tumor cell lines has been widely investigated. However, the molecular mechanisms are uncertain. In this study, we found that exposure of human lung cancer cell lines A549 (p53-wt) and H1299 (p53-depleted) to 8-Cl-Ado induced cell arrest in the G_2/M phase, which was accompanied by accumulation of binucleated and polymorphonucleated cells resulting from aberrant mitosis and failed cytokinesis. Western blotting showed the loss of phosphorylated forms of Cdc2 and Cdc25C that allowed progression into mitosis. Furthermore, the increase in Ser10-phosphorylated histone H3–positive cells revealed by fluorescence-activated cell sorting suggested that the agent-targeted cells were able to exit the G_2 phase and enter the M phase. Immunocytochemistry showed that microtubule and microfilament arrays were changed in exposed cells, indicating that the dynamic instability of microtubules and microfilaments was lost, which may correlate with mitotic dividing failure. Aberrant mitosis resulted in mitotic catastrophe followed by varying degrees of apoptosis, depending on the cell lines. Thus, 8-Cl-Ado appears to exert its cytotoxicity toward cells in culture by inducing mitotic catastrophe.

Neoplasia (2004) **6**, 802–812

Keywords: 8-chloro-adenosine, cytotoxicity, G_2/M arrest, mitotic catastrophe, apoptosis.

Introduction

The essential processes of cell cycle, such as DNA replication, mitosis, and cytokinesis, are triggered by a cell control system. Overexpression of cyclins and suppression of cyclin-dependent kinase (Cdk) inhibitors deregulate Cdk activities and provide cells with a selective growth advantage. Inefficiency of checkpoint control results in initiation of S phase or mitosis despite cellular damage. Thus, specific kinase inhibition and checkpoint activation are commonly considered to be promising targets for antitumor agents [1]. However, the failures of cell cycle arrest responses in tumor cells can also be exploited therapeutically. G_2 checkpoint failure that leads to progression into mitosis prior to DNA damage repair or replication often triggers mitotic catastrophe, which is characterized by mitotic division failure and cell death, by a process that appears to be mechanistically distinct from apoptosis [2–4]. It is believed that cell death through mitotic catastrophe appears to be common in at least some tumors following treatment with chemotherapeutic agents [3], and may be normal response to DNA lesions or incomplete replication at mitosis during development [5,6].

Dynamic instability is an intrinsic property of microtubules and microfilaments, permitting cells to quickly assemble or disassemble cellular filament structures, such as microtubule-based mitotic spindle and microfilament-based contractile ring, to coordinate mitosis and cytokinesis [7]. Therefore, many microtubule-depolymerizing agents and microtubule-polymerizing agents can preferentially disrupt mitosis and induce mitotic catastrophe [3].

The 8-chloro derivative of 8-chloroadenosine 3′,5′-monophosphate (8-Cl-cAMP) is a very potent, site-selective cAMP analogue, whose phase I clinical effects on solid tumors have been evaluated [8,9]. The earlier studies of 8-Cl-cAMP [10,11] and its metabolite, 8-chloro-adenosine (8-Cl-Ado) [10], have demonstrated their potent toxicity for human tumor cells in culture. Cell cycle arrest and apoptotic cell death are considered to be responsible for this effect [9,10,12–18]. Although 8-Cl-cAMP acting through the modulation of protein kinase activities has been reported [12,13,19,20], it seems likely that 8-Cl-cAMP exerts its cytotoxicity by converting into 8-Cl-Ado in living cells [9,10,14–17]. Metabolite analyses, combined with blocking nucleoside uptake, demonstrate that it is 8-Cl-Ado, but not 8-Cl-cAMP, that is phosphorylated to the moiety of

Abbreviations: 8-Cl-Ado, 8-chloro-adenosine; 8-Cl-cAMP, 8-chloroadenosine 3′,5′-monophosphate; 8-Cl-ATP, 8-chloro-adenosine triphosphate; MTT, 3-(4,5-dimethythiazolzyl)-2; 5-diphenyl tetrazolium tromide; PARP, poly (ADP-ribose) polymerase; FACS, fluorescence-activated cell sorting

Address all correspondence to: Hong-Ti Jia, MD, Department of Biochemistry and Molecular Biology, Peking University Health Science Center, Xue Yuan Road 38, Beijing 100083, PR China. E-mail: jiahongti@bjmu.edu.cn

[1]This work was supported in part by National Natural Science Foundation of P. R. China grants 30271448, 30393110, 30471975 and Education Ministry of P. R. China grant 03003.

[2]Hong-Yu Zhang and Yan-Yan Gu contributed equally to this work.

Received 22 March 2004; Revised 5 July 2004; Accepted 6 July 2004.

DOI 10.1593/neo.04247

8-Cl-ATP and mediates tumor cell death through inhibition of RNA synthesis [16,17]. Moreover, there was no evidence that 8-Cl-Ado induces mitotic catastrophe. We describe herein 8-Cl-Ado–induced improper activation of Cdc2 and Cdc25C and aberrant mitotic division. Thus, 8-Cl-Ado appears to exert its cytotoxicity toward cells by inducing G_2/M arrest and triggering mitotic catastrophe followed by apoptosis.

Materials and Methods

Cell Culture and Chemical Treatment

Human lung cancer cell lines A549 (p53-wt) and H1299 (p53-depleted),and leukemia cell lines HL60 and K562 were purchased from ATCC (Rockville, MD). The cells were cultured in RPMI medium 1640 supplemented with 10% fetal bovine serum (GIBCO BRL, Carlsbad, CA), 100 U/ml penicillin, and 100 μg/ml streptomycin, and grown in a 37°C incubator with 5% CO_2.

Twenty-four hours prior to experiments, 1.5×10^6 cells were plated on 75-cm^2 plates for Western blotting, and 5×10^4 cells were plated on coverslips (10 × 10 mm), which were placed in each well of 24-well dishes for immunocytochemical labeling. 8-Cl-Ado (The State Key Laboratory for Natural and Biomimetic Drugs, Peking University HSC, Beijing, China) was dissolved in sterilized 0.85% NaCl solution and added to cultures at the concentration of 2 μM for 24, 48, 72, and 96 hours, respectively. For control experiments, 0.85% NaCl solution was used.

Cell Proliferation Assay

This assay was performed as described previously [21] with slight modifications. Briefly, 24 hours prior to the experiment, the cells were cultured into 96-well dishes (15,000 cells/0.2 ml per well). 8-Cl-Ado of 0, 0.02, 0.2, 2, and 20 μM concentration was added to cultures, respectively, followed by incubation for 24, 48, 72, or 96 hours. Before harvest, 20 μl of MTT [3-(4, 5-dimethythiazolzyl)-2, 5-diphenyl tetrazolium tromide; 5 mg/ml] (Sigma, St. Louis, MO) was added to each well. After incubating for 4 hours, 0.2 ml of DMSO was added to stop reactions. The absorbance values of each well were determined spectrophotometrically at 490 nm on a Microplate Reader (BIO-TEK, Rockville, MA).

Fluorescence-Activated Cell Sorting (FACS)

Cell cycle analysis was performed as previously described [15] with modifications. Briefly, aliquots of cells (1.5×10^6) were pelleted (1500 rpm × 5 minutes at 4°C) and washed twice in ice-cold PBS, and fixed in ice-cold 70% ethanol. For dual-labeling flow cytometry, the fixed cells were incubated with specific anti–Ser10-phosphorylated H3 antibody (Cell Signaling Technology, Beverly, MA) for 30 minutes, followed by incubation with fluorescein isothiocyanate (FITC)–conjugated secondary antibody at room temperature for 30 minutes in the dark. Then the cells were washed in PBS and digested with DNase-free RNase A (10 μg/ml) at 37°C for 30 minutes. Before FACS analysis, the cells ($2 \times l0^4$) were resuspended in 200 μl of propidium iodide (10 μg/ml; Sigma) for DNA staining. A FACScan (Becton Dickinson, Franklin Lakes, NJ) was used to analyze cellular DNA content. For cell cycle analysis, computer programs CELLQuest and ModFit LT 2.0ep for Power were used. Apoptosis was assayed by the appearance of a sub-G_1 (<2*N* ploidy) population by the computer program CELLQuest.

Immunocytochemical Labeling

Immunocytochemical labeling was performed as previously described [22,23] with modifications. Briefly, the cells grown on the coverslips were fixed with 4% formaldehyde (40% formaldehyde and RPMI 1640, 1:9, pH 6.8) at 37°C for 30 minutes, washed in PBS, and then permeabilized with 0.5% Triton X-100 in PBS for 20 minutes at room temperature. After washing in PBS, the cells were washed in a blocking solution consisting of 5% BSA and 0.2% Triton X-100 and stored in the same blocking solution at 4°C until labeling. For tubulin labeling, the fixed cells were incubated for 2 hours at 37°C with a primary rat anti–α-tubulin monoclonal antibody (1:100; Chemicon International, Inc., Temecula, CA) in the blocking solution, followed by three washes in the blocking solution. Then, the cells were incubated with an FITC-conjugated goat antirat IgG (1:l00) (Sino-American Biotech Co., Beijing, China) in the blocking solution for 1 hour at 37°C and subsequently washed three times. These steps were followed by the exposure of the cells to rhodamine phalloidin (1:50) (Molecular Probes, Eugene, OR) in the blocking solution for 40 minutes at 37°C. After that, the cells were incubated for 10 minutes at room temperature with 5 μg/ml Hoechst 33342 (Molecular Probes). After three washes in PBS, the cells were mounted in a 90% glycerol–PBS mixture. Laser confocal microscopy was performed at room temperature using Leica TCS SP2 (Leica Microsystems Heidelberg GmbH, Mannheim, Germany) confocal microscope equipped with a 63 × /1.4 HCxPlanAPO oil immersion objective. Microtubules were excited with an argon laser (488 nm line), microfilaments with a helium–neon laser (543 nm), and DNA with a UV laser (364 nm). Each image represents a two-dimensional maximum projection of sections in the Z-series taken at 0.5-μm intervals across the depth of the cell. Furthermore, a minimum of 50 mitotic cells was counted for each time point for examining chromosome segregation failure and at least 200 interphase cells for examining accumulation of abnormal nuclei.

Western Blotting

Cells were harvested, and proteins were extracted as described previously [24] and quantified with BCA protein assay reagent kit (Pierce, Rockford, IL). Western blotting was performed as described previously [25] with modifications. Cells were lysed with lysis buffer [50 mM Tris–HCl, 250 mM NaCl, 5 mM EDTA, 50 mM NaF, 0.1% Igepal CA-630, and the protease inhibitor cocktail (Roche Diagnostics, Penzberg, Germany)]. Fifty micrograms of total proteins was subjected to SDS-PAGE [10% for phospho-Cdc25C (Ser216),

phospho-Cdc2 (Tyr15), α-tubulin, actin, phospho-Chk2 (Ser19), Cdc25C, Cdc2, and Chk2; 8% for PARP and 12% for caspase-3], transferred onto nitrocellulose membranes, and blocked with 5% nonfat milk in 200 mM NaCl, 25 mM Tris (pH 7.5) and 0.05% Tween 20 at 4°C overnight with rocking. The membranes were probed with specific antibodies for phospho-Cdc25C (Ser216) (1:500), phospho-Cdc2 (Tyr15) (1:500), phospho-Chk2 (Ser19) (1:500), Cdc25C (1:500), Cdc2 (1:500), Chk2 (1:500), tubulin (1:500), actin (1:500), PARP (1:500), or caspase-3 (1:100), respectively. After washing with TBS-T (20 mM Tris, 500 mM NaCl, and 0.1% Tween 20) six times at 5 minutes each, membranes were incubated with horseradish peroxidase–conjugated secondary antibodies [goat antimouse 1:4000 for PARP, caspase-3, rabbit antigoat 1:4000 for actin; goat antirat 1:4000 for tubulin; goat antirabbit 1:1000 for phospho-Cdc25C (Ser216), phospho-Cdc2 (Tyr15), phospho-Chk2 (Ser19), Cdc25C, Cdc2, and Chk2] in TBS containing 0.1% Tween 20 and 1% BSA at room temperature for 1 to 2 hours. Chemiluminescence signals were visualized using Western blotting luminol reagent (Santa Cruz Biotechnology, Santa Cruz, CA) and exposed to film. The antibodies were purchased from Santa Cruz Biotechnology (anti-PARP, F-2; antiactin, I-19), Oncogene Research Products (Darmstadt, Germany; anti-caspase-3, Ab-I), Cell Signaling Technology [anti-Cdc25C and phospho-Cdc25C (Ser216), Cdc2 and phospho-Cdc2 (Tyr15), and Chk2 and phospho-Chk2 (Ser19)], and Chemicon International, Inc. (antitubulin).

Results

Growth Inhibition and G_2/M Arrest

As revealed by the time–effect and dose–effect curves, 8-Cl-Ado (≥2 μM) caused significant growth inhibition of A549 and H1299 cells within 24 to 96 hours after exposure (Figure 1). We also assessed the ability of 8-Cl-Ado to inhibit the growth of leukemia cells (data not shown). There appeared to be a little quantitative difference in the inhibitory effects of 8-Cl-Ado on cell growth, depending on time, dose, and tumor cell lines.

To determine whether the inhibition of cell growth by 8-Cl-Ado was closely related to cell cycle control, we analyzed the cell cycle distribution of the tumor cells with FACS. As shown in Figure 2 *A*, exposure of A549 cells to 2 μM 8-Cl-Ado caused increases from 14.49% to 34.68% of G_2/M subpopulation within 24 to 96 hours, compared with unexposed cells that showed 10.15% G_2/M subpopulation. In H1299 cells, 8-Cl-Ado–induced accumulation of G_2/M phase was 18.4% in 24 hours, 22.57% in 48 hours, 30.07% in 72 hours, and 27.32% in 96 hours, respectively, compared with 18.89% G_2/M in unexposed cells. Compared with 8.15% G_2/M phase in unexposed cells, exposed K562 cells in G_2/M phase showed 6.23% to 31.14% increase in 24 to 72 hours. All of them showed a time-dependent increase in G_2/M subpopulation within 24 to 96 hours. Similar G_2/M distributions in three cell lines were detected in dose–response experiments (Figure 2 *B*). However, G_2/M population in HL60 cells had no any changes within 24 to 72 hours, compared with unexposed cells. These results indicate that 8-Cl-Ado induces cell accumulation in G_2/M phase in a time-, dose- and cell type–dependent manner. We noted that 8-Cl-Ado could induce apoptosis in varying degrees in target cells, depending on cell lines.

Because site-specific phosphorylation of histone H3 is a marker for mitotic progression in mammalian cells [26], we analyzed Ser10-phospho-H3 by FACS (Figure 3 *A*). In A549 cells, 24 to 96 hours of 8-Cl-Ado exposure induced 10% to 15% phospho-H3–positive cells, compared with 3% positive staining in unexposed cells. H1299 cells showed 12% to 16% phospho-H3 staining after 24 to 96 hours of exposure, whereas unexposed cells had 2% positive cells. PI staining showed phospho-H3–positive cells with 4*N* DNA. These data indicate that 8-Cl-Ado–exposed cells are able to enter the M phase and arrest there, which contributes in part to cells accumulating in G_2/M phases.

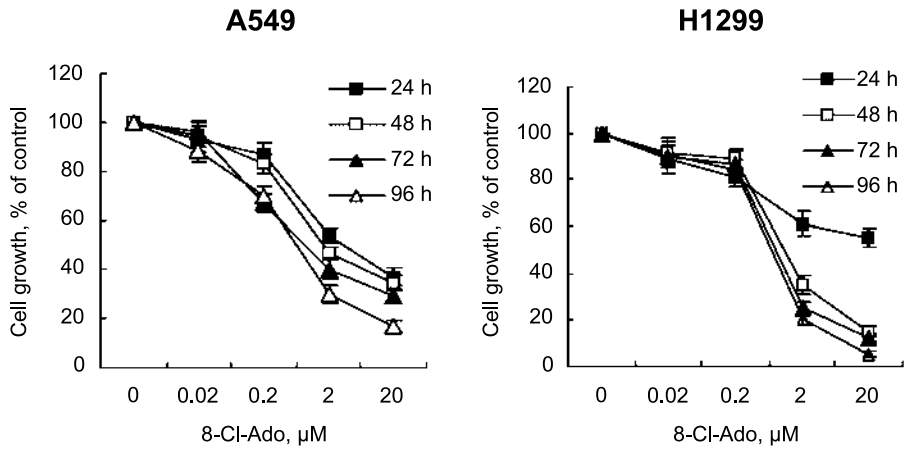

Figure 1. *Effects of 8-Cl-Ado on cell proliferation. A549 and H1299 cells were exposed to 8-Cl-Ado at the indicated concentrations for 24, 48, 72, or 96 hours, respectively. Cell proliferation was evaluated with MTT assay (see Materials and Methods section). Data represent mean ± SD derived from three independent experiments.*

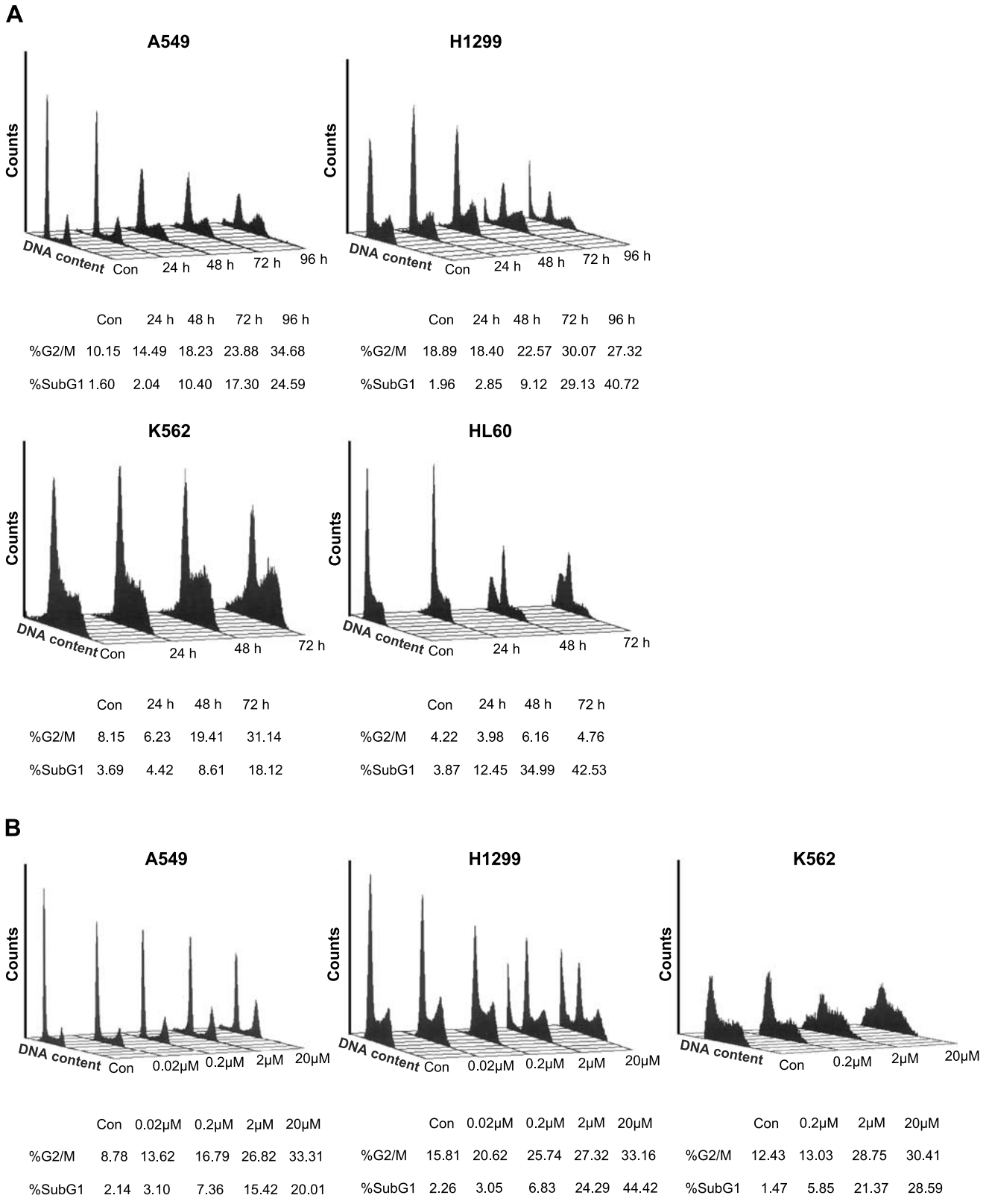

	Con	24 h	48 h	72 h	96 h
%G2/M	10.15	14.49	18.23	23.88	34.68
%SubG1	1.60	2.04	10.40	17.30	24.59

	Con	24 h	48 h	72 h	96 h
%G2/M	18.89	18.40	22.57	30.07	27.32
%SubG1	1.96	2.85	9.12	29.13	40.72

	Con	24 h	48 h	72 h
%G2/M	8.15	6.23	19.41	31.14
%SubG1	3.69	4.42	8.61	18.12

	Con	24 h	48 h	72 h
%G2/M	4.22	3.98	6.16	4.76
%SubG1	3.87	12.45	34.99	42.53

	Con	0.02μM	0.2μM	2μM	20μM
%G2/M	8.78	13.62	16.79	26.82	33.31
%SubG1	2.14	3.10	7.36	15.42	20.01

	Con	0.02μM	0.2μM	2μM	20μM
%G2/M	15.81	20.62	25.74	27.32	33.16
%SubG1	2.26	3.05	6.83	24.29	44.42

	Con	0.2μM	2μM	20μM
%G2/M	12.43	13.03	28.75	30.41
%SubG1	1.47	5.85	21.37	28.59

Figure 2. *Analyses of cell cycle. (A) Time–response experiments. The A549, H1299, K562, and HL 60 cells were exposed to 2 μM 8-Cl-Ado for 24, 48, 72, or 96 hours, respectively. The cells were stained with PI and DNA content was analyzed by FACScan as described in Materials and Methods section. Con: unexposed cells (control). (B) Dose–response experiments. The A549, H1299, and K562 cells were exposed to 8-Cl-Ado (0.02, 0.2, 2, or 20 μM) for 72 hours, respectively. G_2/M population and apoptosis (%) are listed on the bottom. Apoptosis is revealed by sub-G_1 (<2N ploidy). Data represent one of three independent experiments.*

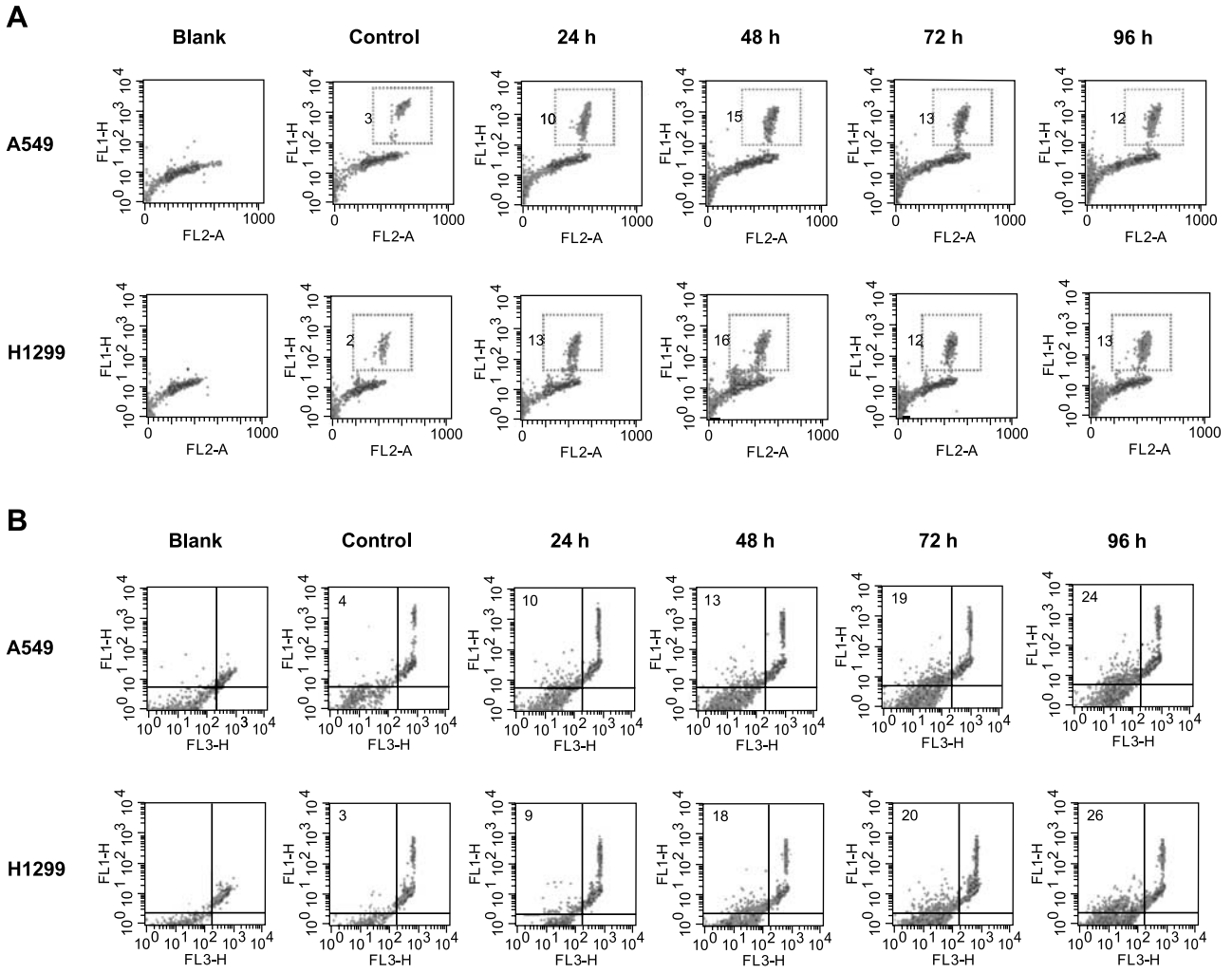

Figure 3. *Analyses of mitotic progression. (A) Phospho-histone H3 as a marker for mitotic progression. After exposure to 8-Cl-Ado (2 μM) for an indicated time, the cells were fixed with 70% ethanol; stained with anti–Ser10-phospho-H3 primary antibody, FITC-conjugated secondary antibody, and PI; and analyzed by FACScan. PI and FITC signals were measured in linear mode FL2-A and in logarithmic mode FL1-H, respectively. No primary antibody was used in the "blank"; dual staining of unexposed cells was used as control. The mitotic cells in red square are positive for phospho-H3. (B) Apoptosis analysis. Cell exposure and staining are the same as in (A). PI and FITC signals were recorded in logarithmic mode FL3-H and FL1-H, respectively. The cells in the left quadrants are apoptotic cells with <2N DNA content; that in the left upper quadrant are phospho-H3–positive. The values (%) represent means of two independent experiments. Data represent one of two independent experiments.*

G_2 Checkpoint Failure

Because Cdc2 and Cdc25C activities are essential for G_2/M transition [27–29], we performed Western blotting with phospho-Cdc25C (Ser216) and phospho-Cdc2 (Tyr15) antibodies (Figure 4). In comparison with unexposed cells, markedly decreased Ser216-phospho-Cdc25C and Tyr15-phospho-Cdc2 were detected in exposed A549 cells within 24 to 96 hours. In exposed H1299 cells, Ser216-phospho-Cdc25C partially decreased in 24 hours and almost completely disappeared within 48 to 96 hours; Tyr15-phospho-Cdc2 was markedly decreased within 24 to 72 hours and slightly decreased in 96 hours. These results indicate a G_2 checkpoint failure in both exposed cell lines, marked by the loss of phosphorylated forms of Cdc2 and Cdc25C.

To further check the loss of phosphorylated proteins, we determined Ser19-phospho-Chk2 with specific antibody. We found that Chk2 was constitutively phosphorylated at Ser19 in unexposed cells. By contrast, Ser19-phospho-Chk2 in exposed A549 cells was considerably decreased within 24 to 96 hours (Figure 4). In exposed H1299 cells, phospho-Chk2 was also decreased, although it was not so exciting. These data suggest that 8-Cl-Ado may inhibit phosphorylation in target cells.

Mitotic Catastrophe

G_2 checkpoint failure promotes mitotic catastrophe [3]. We thus examined the mitotic division using immunocytochemistry method. The confocal micrographs showed a part of the mitotic course of A549 cells (Figure 5). In control cells, mitotic cells underwent the normal mitosis (Figure 5 *A*, *a–c*). 8-Cl-Ado–exposed cells, however, displayed aberrant mitosis (Figure 5 *A*, *d–f*). In an abnormal metaphase in exposed cells, the chromosomes did not align properly, and there were several clusters of decondensed chromosomes distributed randomly (Figure 5 *A*, *d*). In an abnormal anaphase,

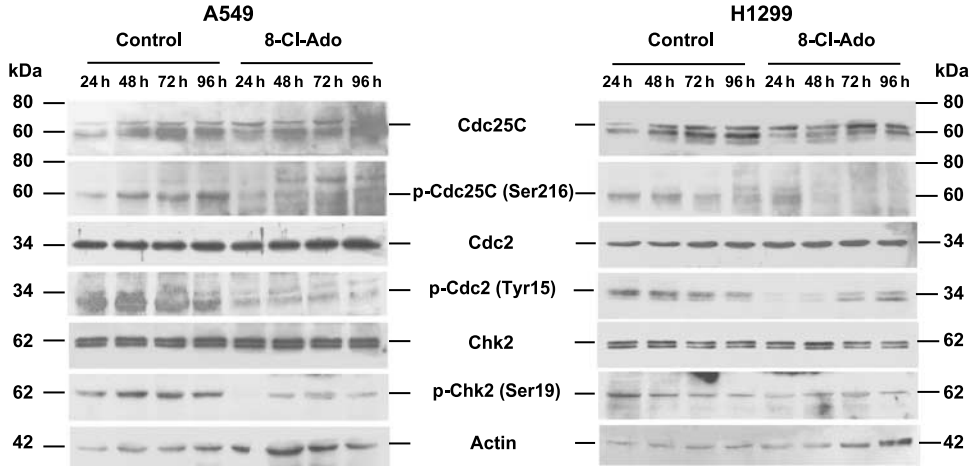

Figure 4. *8-Cl-Ado–induced G_2 checkpoint failure. The A549 and H1299 cells were cultured, and unexposed (Control) or exposed to 2 μM 8-Cl-Ado for 24, 48, 72, or 96 hours, respectively. Cell extracts were prepared and Western blotting analyses were performed for Cdc25C, phospho-Cdc25C (Ser216), Cdc2, phospho-Cdc2 (Tyr15), Chk2, and phospho-Chk2 (Ser19) (see Materials and Methods section). Fifty micrograms of proteins was loaded for each lane, and the antigen–antibody complex was visualized by chemiluminescence. Actin was used as control.*

the chromosomes decondensed unusually and were divided asymmetrically and incompletely (Figure 5 *A*, *e*), indicating the lagging anaphase and chromosome segregation failure. In a cell with failed cytokinesis, two daughter nuclei were linked by residual chromatin bridge, the disruption of microtubule and microfilament networks could be perceived, and the microfilament-based contractile ring could not form (Figure 5 *A*, *f*). Based on the observation of mitosis, the frequency of failed mitosis was calculated (Figure 5 *B*): the proportion of failed mitotic cells in exposed A549 cells was 32% to 45% (control was 11%) and that in H1299 cells was 24% to 33% (control was 6%) in 24 to 96 hours, respectively. These results demonstrate that 8-Cl-Ado can interfere with mitosis and cytokinesis in both cells and induce mitotic catastrophe.

Binuclei and Multinuclei Accumulation and Filament Network Disturbance

Because mitotic catastrophe often results from aberrant mitosis [3], and microtubules and microfilaments are essential for cell division [7,23,30], triple fluorescence labeling was employed to analyze the nuclear and cellular morphology and the microtubule and microfilament organization following 8-Cl-Ado exposure (Figure 6, *A*–*D*). In control systems, most unexposed A549 and H1299 cells were characterized by single nucleus. When exposed A549 cells to 8-Cl-Ado (2 μM), more than 20% of the cells with binuclei, polymorphonuclei, and multinuclei accumulated by 24 hours; this ratio increased to about 25.5% to 38% within 48 to 96 hours; about 3.5% to 12% A549 cells with shrunken bodies and condensed or fragmented nuclei could be perceived in 48 to 96 hours (Figure 6 *E*). In H1299 cells, the maximum accumulation of binuclei, polymorphonuclei, and multinuclei was 27.5% by 96 h; the shrunken H1299 cells with condensed or fragmented nuclei increased from 4% to 24% within 24 to 96 hours (Figure 6 *F*). These results further demonstrate that 24 to 96 hours of 8-Cl-Ado exposure may induce dividing failure and mitotic catastrophe.

Both unexposed A549 and H1299 cells (controls in Figure 6, *A*–*D*) had the typical fibrillar arrays of interphase microtubules revealed by anti–α-tubulin antibody: the microtubule spokes radiated from a central site occupied by centrosome, the primary microtubule-organizing center (MTOC). In exposed A549 (Figure 6, *A* and *B*) and H1299 cells (Figure 6, *C* and *D*), however, the microtubules were disorganized by 24 hours. Going along with the time, the alteration grew obviously. Microfilaments were also disturbed in 24 to 48 hours in both cell lines. These data suggest that 8-Cl-Ado can perturb the dynamic instability of cellular microtubules and microfilaments, which may interfere with mitosis and lead to mitotic catastrophe.

Long Exposure–Induced Apoptosis

To evaluate apoptosis after 8-Cl-Ado exposure, several methods including DNA fragmentation, FACS, and Hoechst staining were employed. It was easy to get a DNA ladder with 8-Cl-Ado–treated HL60 cells in 24 hours, but failed to do so with A549, H1299, and K562 cell lines during all tested time (data not shown). In FACS assays (Figure 2), the A549, H1299, and K562 cells increased sub-G_1 DNA content characterizing apoptosis after 48 to 96 hours of exposure. Our results indicate that 8-Cl-Ado long exposure can induce apoptosis.

To determine whether the cells undergoing apoptosis were recruited from mitosis, phosphorylated H3–positive cells were analyzed by FACS. Compared with unexposed A549 and H1299 cells that showed 3% and 2% positive staining for Ser10-phospho-H3, 8-Cl-Ado exposure for 48 to 96 hours induced 13% to 24% and 18% to 26% phospho-H3

positivity in A549 and H1299 apoptotic cells, respectively (Figure 3 *B*), indicating that apoptosis at least in part came from mitosis.

Because caspase-3 pathway is commonly implicated in apoptosis, we next performed Western blotting to test the activation of caspase-3 and the cleavage of its substrate, poly (ADP-ribose) polymerase (PARP). In exposed H1299 cells, the active caspase-3 subunit p17 was detected within 24 to 96 hours, and a p85 fragment was yielded by PARP (p115) after 48 to 96 hours of exposure (Figure 7). However, the degradation of PARP without the activation of caspase-3 was detected in A549 cells after 48 to 96 hours of exposure. These suggest that 8-Cl-Ado–induced apoptosis proceeds through or bypasses caspase-3 activation, depending on cell lines.

Discussion

In this study, we demonstrate that 8-Cl-Ado can induce G_2 checkpoint failure and chromosome segregation failure. G_2 checkpoint failure is due to the loss of phosphorylated forms of Cdc2. Chromosome segregation failure may correlate with the loss of dynamic instability of microtubules and microfilaments. Aberrant mitosis results in mitotic catastrophe

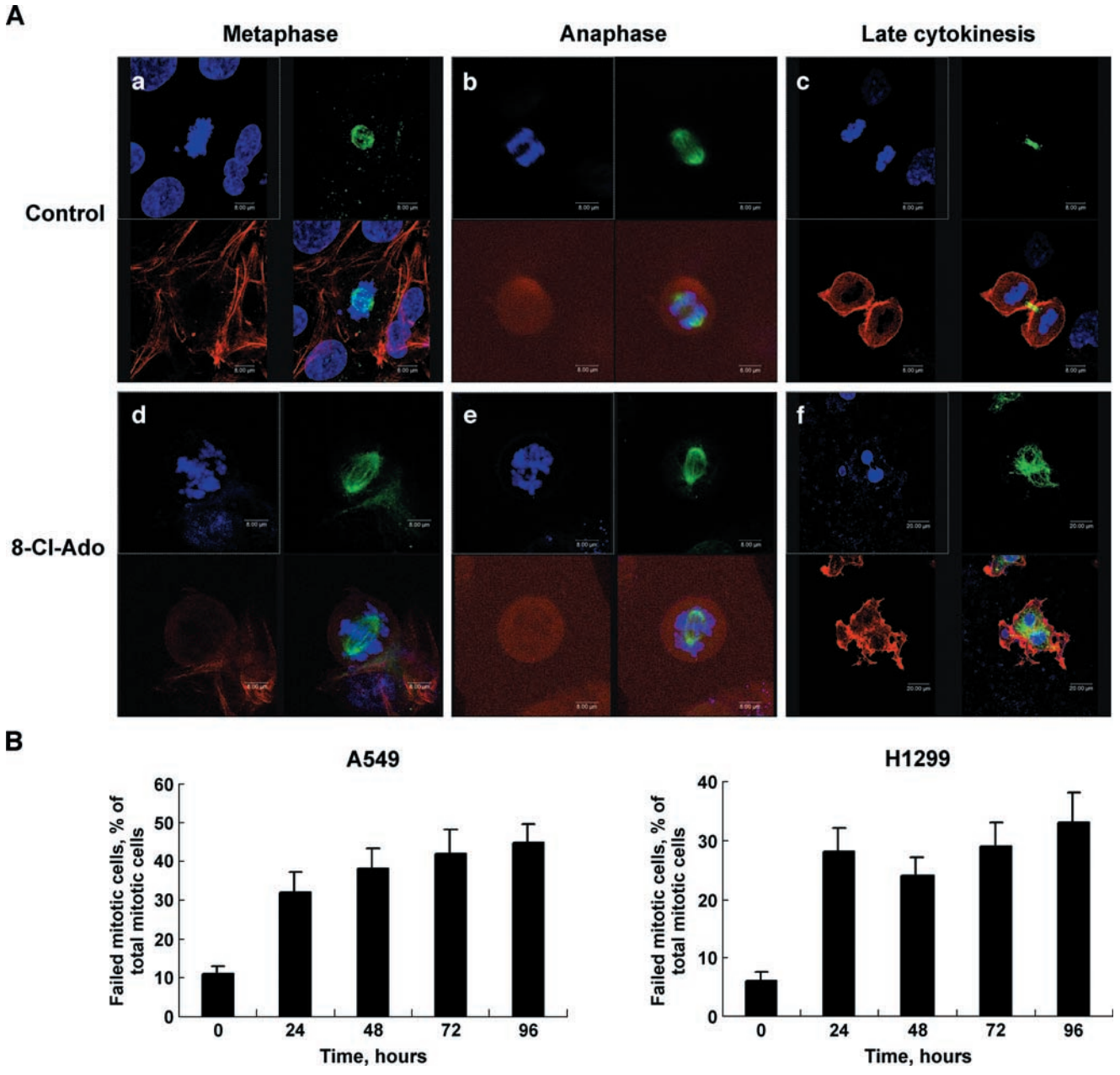

Figure 5. *8-Cl-Ado–induced chromosome segregation failure. Cells were unexposed or exposed to 8-Cl-Ado (2 μM) for 24 to 96 hours. Immunocytochemistry was performed as described in Materials and Methods section. The cells were examined with confocal microscope. (A) Photographs characteristic of mitotic division of A549 cells unexposed (a–c) (control) or exposed to 8-Cl-Ado (d–f). Tubulin is labeled with green, actin with red, and DNA with blue. (B) Histograms showing the percentage of failed mitotic cells relative to the total mitotic cells in A549 and H1299 cells, respectively. Data represent mean ± SD derived from three independent experiments.*

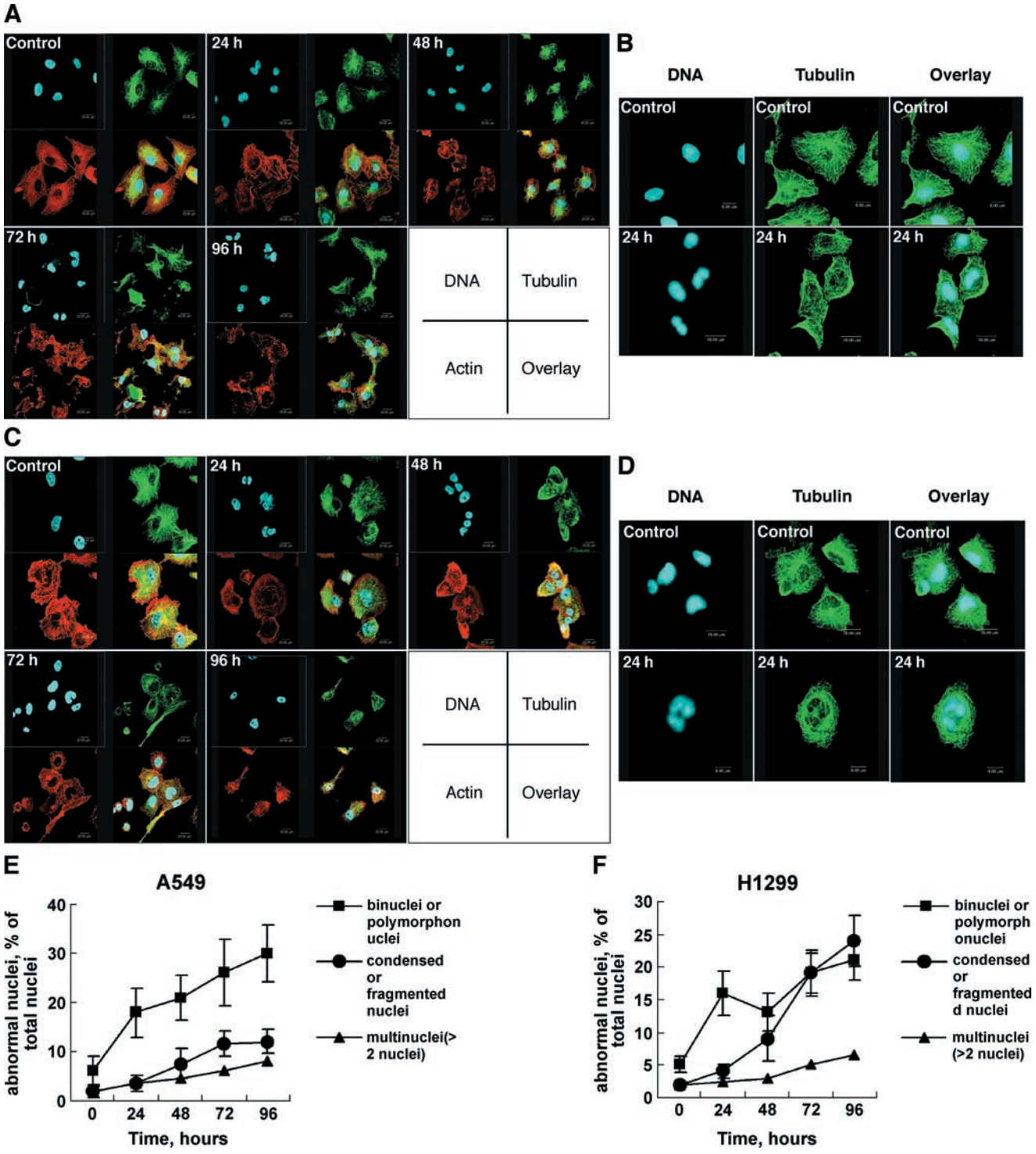

Figure 6. *Accumulation of abnormal nuclei and disturbance of microtubule and microfilament network. A549 (A and B) and H1299 (C and D) cells were exposed to 2 μM 8-Cl-Ado for 24, 48, 72, or 96 hours, respectively, and immunocytochemistry as described in Materials and Methods section. The cells were examined with a confocal microscope. Tubulin is stained with green, actin with red, and DNA with blue. The enlarged photographs of A549 (B) and H1299 (D) are presented. Cells mock-exposed for 96 and 24 hours were used as "control" in (A) and (C), and (B) and (D), respectively. (E and F) Histograms showing the percentage of abnormal nuclei relative to the total nuclei in A549 and H1299 cells, respectively. Binuclei, polymorphonuclei, and multinuclei were considered to be abnormal nuclei. Data represent mean ± SD derived from three independent experiments.*

followed by apoptosis in 8-Cl-Ado–exposed cells, depending on the cell lines.

Although accumulation of cells in S phase and G_2/M phases induced by 8-Cl-Ado or 8-Cl-cAMP has been reported [10,12,13], molecular mechanisms are uncertain. We showed that exposure of human tumor cells to 8-Cl-Ado accumulated the subpopulation of G_2/M cells in a time-, dose-, and cell type–dependent manner. Compared with unexposed cells, 8-Cl-Ado exposure induced three- to five-fold and six- to eight-fold increases in phospho-H3–positive

cells in A549 and H1299 cell lines, respectively, suggesting that 8-Cl-Ado–exposed cells are able to enter the M phase. Entry of all eukaryotic cells into the M phase of the cell cycle is regulated by activation of Cdc2 kinase. Activation of Cdc2 (Tyr15 dephosphorylation) is carried out by Cdc25C phosphatase [28,31,32]. In this study, we found the loss of phosphorylated forms of Cdc25C and Cdc2 in 8-Cl-Ado–exposed cells, which may associate with G_2 checkpoint failure.

It has been well established that 8-Cl-Ado can convert to 8-Cl-ATP and inhibit mRNA synthesis in target cells by transcriptional termination [16,17]. Therefore, it is possible that 8-Cl-Ado reduces the expression of genes including Cdc2, Cdc25C, and Chks in G_2/M checkpoint pathways. It is also possible that 8-Cl-Ado inhibits ATP-dependent reactions in target cells by interfering with ATP generation or kinase activity. Both molecular ways may contribute to the loss of the phosphorylated forms of Cdc2, Cdc25C, and Chks in 8-Cl-Ado–exposed cells. Alternatively, the loss of phosphorylated proteins may be independent of checkpoint cascade pathway. We thus suggest that 8-Cl-Ado may induce G_2 checkpoint failure, which is directly associated with the loss of phosphorylated Cdc2 in exposed cells. Unsurprisingly, no gross changes in total proteins of Cdc2, Cdc25C, and Chk2 as well as actin (control) in exposed cells were detected by Western blotting because the same amount of proteins was routinely used for this assay and the syntheses of all mRNA/protein species were inhibited by 8-Cl-Ado. Therefore, our results do not exclude the notion that 8-Cl-Ado inhibits RNA/protein syntheses in exposed cells.

It is clear that cell cycle checkpoints prevent or delay mitosis in damaged cells [33–36]. G_2/M checkpoint failures that lead to progression into mitosis prior to DNA damage repair or replication often trigger mitosis catastrophe [3]. Microtubule-targeting agents can also cause mitotic catastrophe [3,33,37]. In mitotic division analyses, we found aberrant mitotic division and failed cytokinesis in 8-Cl-Ado–exposed cells. Aberrant division may result from disturbance of microtubule and actin filament structures. At present, we have no direct evidence that the cellular filaments are primary targets for 8-Cl-Ado. It is possible that 8-Cl-Ado may directly or indirectly perturb the functions of the microtubule-based mitotic spindle and the actin-based contractile ring by interfering with ATP metabolism. Metabolite analyses have demonstrated that exposure of 8-Cl-Ado accumulates monophosphates and triphosphates of 8-Cl-Adenosine in living cells [16]. Therefore, the depletion of cellular ATP pool may play an essential role in 8-Cl-Ado–mediated cytotoxicity.

There are possible explanations for the mechanisms by which 8-Cl-Ado perturbs the dynamic instability of the cellular filaments, which may correlate with mitotic dividing failure. First, the decrease in ATP synthesis may block the transfer of γ-phosphate from ATP to GDP for generating GTP. The reorganization of microtubule may be inhibited because the hydrolysis of GTP bound to tubulin is the heart of the rapid turnover of microtubules [30,38]. Second, the depletion of ATP may suppress the conversion of chemical energy into mechanical work. ATP hydrolysis by kinesin is tightly coupled to generating force, by which vesicles and beads can move toward the plus end of microtubules during mitosis [7,30,39,40]. Third, the elimination of ATP pool by 8-Cl-Ado may directly block ATP-dependent association/dissociation reactions at the ends of the actin, and thereby make dynamic instability and treadmilling impossible. In addition, 8-Cl-ATP, as an ATP analogue, may competitively bind to the ATP-binding site on actin filaments, inhibiting their polymerization. The mechanism by which 8-Cl-Ado affects the dynamic instability of the cellular filaments needs to be further determined.

Cell death through mitotic catastrophe appears to be common in some tumors following treatment with chemotherapeutic agents [3]. Until now, mitotic catastrophe is defined mostly by morphology. Some studies suggest that mitotic catastrophe shares some common pathways with apoptosis, whereas more evidences show that it is independent of apoptosis [3,37]. It has been reported that a variety of tumor cells exposed to 8-Cl-Ado died by apoptosis [9,12,13,15,16]. However, no study of mitotic catastrophe induced by 8-Cl-Ado has been described. In this study, we could hardly detect apoptosis in A549, H1299, and K562 cells by DNA ladder in

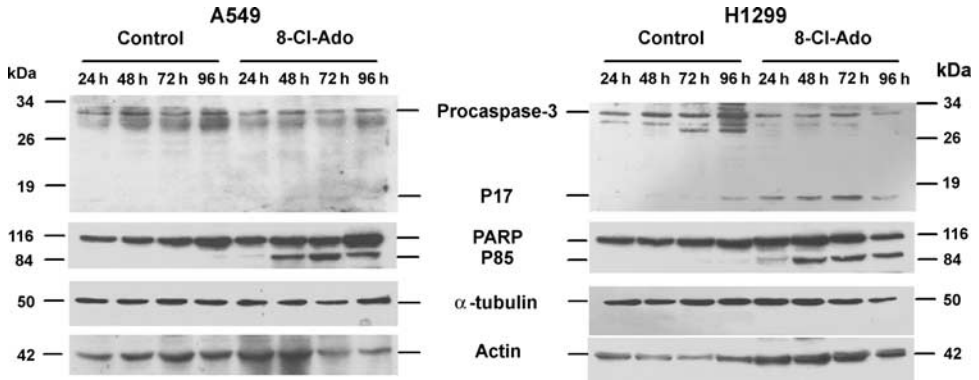

Figure 7. *8-Cl-Ado–induced apoptosis way. A549 and H1299 cells were unexposed (control) or exposed to 8-Cl-Ado (2 μM) for 24, 48, 72, or 96 hours. After harvest, cell extracts were prepared, and the activation of caspase-3 and the cleavage of PARP were examined by Western blotting as described in Materials and Methods section. Actin and tubulin were used as controls.*

all tested times (24–96 hours), except HL60 cells; the sub-G_1 cells could be identified by FACS only after long exposure (>48 hours). These facts indicate that apoptosis is a late event in 8-Cl-Ado–exposed cells. In contrast, binuclei and polymorphonuclei and multinuclei initially accumulated in the cultures by 24 hours, suggesting that mitotic catastrophe is an early and major event after 8-Cl-Ado exposure. H3 phosphorylation is a marker for mitotic progression [26]. We found that Ser10-phospho-H3–positive cells in apoptotic population were markedly increased in 8-Cl-Ado–exposed cells. This fact suggests that the cells undergoing apoptosis may recruit at least in part from mitosis as a consequence of mitotic catastrophe. Evaluation of the effects of 8-Cl-Ado on several tumor cell lines including A549, H1299, K562, $HepG_2$ (data not shown), and HL60 cells showed that most of them arrested in G_2/M phase and underwent mitotic catastrophe followed by varying degrees of apoptosis, except HL60 cells that died by apoptosis without G_2/M arrest. Our results support the notion that cell death through mitotic catastrophe appears to be common in at least some tumors following treatment with chemotherapeutic agents [3]. Our study also suggests that 8-Cl-Ado induces G_2/M arrest and mitotic catastrophe of target cells followed by apoptosis, depending on cell lines. Whether our proposed mechanism of cell death is valid for a wide variety of cancer cells deserves further studied.

Acknowledgements

We thank Bin Xue (Department of Neurobiology, PUHSC, China) and Jun-Jun Xiao (Department of Cell Biology, PUHSC, China) for their assistance with immunocytochemistry. We thank Li-He Zhang (School of Pharmaceutics, Peking University, China) for kindly providing 8-Cl-Ado.

References

[1] Hartwell LH and Kastan MB (1994). Cell cycle control and cancer. *Science* **266,** 1821–1828.

[2] Shapiro GI and Harper JW (1999). Anticancer drug targets: cell cycle and checkpoint control. *J Clin Invest* **104,** 1645–1653.

[3] Roninson IB, Broude EV, and Chang BD (2001). If not apoptosis, then what? Treatment-induced senescence and mitotic catastrophe in tumor cells. *Drug Resist Updat* **4,** 303–313.

[4] Raff JW (2003). Cell division: genome maintenance. *Nature* **423,** 493–495.

[5] Sibon OC, Kelker A, Lemstra W, and Theurkauf WE (2000). DNA-replication/DNA-damage–dependent centrosome inactivation in *Drosophila* embryos. *Nat Cell Biol* **2,** 90–95.

[6] Takada S, Kelkar A, and Theurkauf WE (2003). *Drosophila* checkpoint kinase 2 couples centrosome function and spindle assembly to genomic integrity. *Cell* **113,** 87–99.

[7] Scholey JM, Brust-Mascher I, and Mogilner A (2003). Cell division. *Nature* **422,** 746–752.

[8] Tortora G, Ciardiello F, Pepe S, Tagliaferri P, Ruggiero A, Bianco C, Guarrasi R, Miki K, and Bianco AR (1995). Phase I clinical study with 8-chloro-cAMP and evaluation of immunological effects in cancer patients. *Clin Cancer Res* **1,** 377–384.

[9] Halgren RG, Traynor AE, Pillay S, Zell JL, Heller KF, Krett NL, and Rosen ST (1998). 8Cl-cAMP cytotoxicity in both steroid sensitive and insensitive multiple myeloma cell lines is mediated by 8Cl-adenosine. *Blood* **92,** 2893–2898.

[10] Langeveld CH, Jongenelen CAM, Heimans JJ, and Stoof JV (1991). Growth inhibition of human glioma cells induced by 8-chloroadenosine, an active metabolite of 8-chlorocyclic adenosine 3′,5′-monophosphate. *Cancer Res* **51,** 6207–6208.

[11] Ally S, Clair T, Katsaros D, Tortora G, Yokozaki H, Finch RA, Avery TL, and Cho-Chung YS (1989). Inhibition of growth and modulation of gene expression in human lung carcinoma in athymic mice by site-selective 8-Cl-cyclic adenosine monophosphate. *Cancer Res* **49,** 5650–5655.

[12] Kim SN, Ahn YH, Kim SG, Park SD, Cho-Chung YS, and Hong SH (2001). 8-Cl-cAMP induces cell cycle–specific apoptosis in human cancer cells. *Int J Cancer* **93,** 33–41.

[13] Grbovic O, Jovic V, Ruzdijic S, Pejanovic V, Rakic L, and Kanazir S (2002). 8-Cl-cAMP affects glioma cell-cycle kinetics and selectively induces apoptosis. *Cancer Invest* **20,** 972–982.

[14] Taylor CW and Yeoman LC (1992). Inhibition of colon tumor cell growth by 8-chloro-cAMP is dependent upon its conversion to 8-chloro-adenosine. *Anticancer Drugs* **3,** 485–491.

[15] Carlson CC, Chinery R, Burnham LL, and Dransfield DT (2000). 8-Cl-Adenosine–induced inhibition of colorectal cancer growth *in vitro* and *in vivo*. *Neoplasia* **2,** 441–448.

[16] Gandhi V, Ayres M, Halgren RG, Krett NL, Newman RA, and Rosen ST (2001). 8-Chloro-cAMP and 8-chloro-adenosine act by the same mechanism in multiple myeloma cells. *Cancer Res* **61,** 5474–5479.

[17] Stellrecht CM, Rodriguez C Jr, Ayres M, and Gandhi V (2003). RNA-directed actions of 8-chloro-adenosine in multiple myeloma cells. *Cancer Res* **63,** 7968–7974.

[18] Chen LS and Sheppard TL (2002). Synthesis and hybridization properties of RNA containing 8-chloroadenosine. *Nucleosides Nucleotides Nucleic Acids* **21,** 599–617.

[19] Rohlff C, Clair T, and Cho-Chung YS (1993). 8-Cl-cAMP induces truncation and down-regulation of the RI alpha subunit and up-regulation of the RII beta subunit of cAMP-dependent protein kinase leading to type II holoenzyme–dependent growth inhibition and differentiation of HL-60 leukemia cells. *J Biol Chem* **268,** 5774–5782.

[20] Lange-Carter CA, Vuillequez JJ, and Malkinson AM (1993). 8-Chloro-adenosine mediates 8-chloro-cyclic AMP–induced down-regulation of cyclic AMP–dependent protein kinase in normal and neoplastic mouse lung epithelial cells by a cyclic AMP–independent mechanism. *Cancer Res* **53,** 393–400.

[21] Li S-Y, Ni J-H, Xu D-S, and Jia H-T (2003). Down-regulation of GluR2 is associated with Ca^{2+}-dependent protease activities in kainite-induced apoptotic cell death in cultured rat hippocampal neurons. *Neurosci Lett* **352,** 105–108.

[22] Yamazaki Y, Tsuruga M, Zhou D, Fujita Y, Shang X, Dang Y, Kawasaki K, and Oka S (2000). Cytoskeletal disruption accelerates Caspase-3 activation and alters the intracellular membrane reorganization in DNA damage-induced apoptosis. *Exp Cell Res* **259,** 64–78.

[23] Canman JC, Cameron LA, Maddox PS, Straight A, Tirnauer JS, Mitchison TJ, Fang G, Kapoor TM, and Salmon ED (2003). Determining the position of the cell division plane. *Nature* **424,** 1074–1078.

[24] Zhu WG, Lakshmanan R, Beal MD, and Otterson GA (2001). DNA methyltransferase inhibition enhances apoptosis induced by histone deacetylase inhibitors. *Cancer Res* **61,** 1327–1333.

[25] Gong M, Ni J-H, and Jia H-T (2002). Increased exchange rate of histone H1 on chromotin by exogenous myogenin expression. *Cell Res* **12,** 395–400.

[26] Hendzel MJ, Wei Y, Mancini MA, Van Hooser A, Ranalli T, Brinkley BR, Bazett-Jones DP, and Allis CD (1997). Mitosis-specific phosphorylation of histone H3 initiates primarily within pericentromeric heterochromatin during G2 and spreads in an ordered fashion coincide with mitotic chromosome condensation. *Chromosoma* **106,** 348–360.

[27] Nilsson I and Hoffmann I (2000). Cell cycle regulation by the Cdc25 phosphatase family. *Prog Cell Cycle Res* **4,** 107–114.

[28] Bulavin DV, Higashimoto Y, Popoff IJ, Gaarde WA, Basrur V, Potapova O, Appella E, and Fornace AJ Jr (2001). Initiation of G2/M checkpoint after ultraviolet radiation requires p38 kinase. *Nature* **411,** 102–107.

[29] Pines J (1999). Four-dimensional control of the cell cycle. *Nat Cell Biol* **1,** E73–E79.

[30] Howard J and Hyman AA (2003). Dynamics and mechanics of the microtubule plus end. *Nature* **422,** 753–758.

[31] Harvey S, Decker R, Dai Y, Schaefer G, Tang L, Kramer L, Dent P, and Grant S (2001). Interactions between 2-fluoroadenine 9-β-D-arabinofuranoside and the kinase inhibitor UCN-01 in human leukemia and lymphoma cells. *Clin Cancer Res* **7,** 320–330.

[32] Iliakis G, Wang YA, Guan J, and Wang H (2003). DNA damage checkpoint control in cells exposed to ionizing radiation. *Oncogene* **22,** 5834–5847.

[33] Jordan MA and Wilson L (1999). The use and action of drugs in analyzing mitosis. *Methods Cell Biol* **61,** 267–295.

[34] Sato N, Mizumoto K, Nakamura M, and Tanaka M (2000). Radiation-induced centrosome overduplication and multiple mitotic spindles in human tumor cells. *Exp Cell Res* **255,** 321–326.

[35] Scolnick DM and Halazonetis TD (2000). Chfr defines a mitotic stress checkpoint that delays entry into metaphase. *Nature* **406,** 430–435.

[36] Tokuyama Y, Henning HF, Kawamura K, Tarapore P, and Fukasawa K (2001). Specific phosphorylation of nucleophosmin on Thr199 by CDK2/cyclin E and its role in centrosome duplication. *J Biol Chem* **276,** 21529–21537.

[37] Nabha SM, Mohammad RM, Dandashi MH, Coupaye-Gerard B, Aboukameel A, Pettit GR, and Al-Katib AM (2002). Combretastatin-A4 prodrug induces mitotic catastrophe in chronic lymphocytic leukemia cell line independent of caspase activation and poly (ADP-ribose) polymerase cleavage. *Clin Cancer Res* **8,** 2735–2741.

[38] Hyman AA, Chretien D, Arnal I, and Wade RH (1995). Structural changes accompanying GTP hydrolysis in microtubules: information from a slowly hydrolyzable analogue guanylyl-(alpha,beta)-methylene-diphosphonate. *J Cell Biol* **128,** 117–125.

[39] Walczak CE, Vernos I, Mitchison TJ, Karsenti E, and Heald R (1998). A model for the proposed roles of different microtubule-based motor proteins in establishing spindle bipolarity. *Curr Biol* **8,** 903–913.

[40] Kim AJ and Endow SA (2000). A kinesin family tree. *J Cell Sci* **113,** 3681–3682.